J. Biochem. **140**, 851–859 (2006)
doi:10.1093/jb/mvj218

Inhibitory Activity of 1-Farnesylpyridinium on the Spatial Control over the Assembly of Cell Wall Polysaccharides in *Schizosaccharomyces pombe*

Masahiro Hamada[1,*], Ikumi Ohata[1], Ken-ichi Fujita[1], Yoshinosuke Usuki[1], Akira Ogita[2], Junpei Ishiguro[3] and Toshio Tanaka[1,†]

[1]Graduate School of Science and [2]Research Center for Urban Health and Sports, Osaka City University, 3-3-138 Sugimoto, Sumiyoshi-ku, Osaka 558-8585; and [3]Department of Biology, Faculty of Science and Engineering, Konan University, Okamoto 8-9-1, Kobe 658-8501

Received October 10, 2006; accepted October 31, 2006

The modes of actions of 1-farnesylpyridinium (FPy) on yeast cell growth were investigated on the basis of its effects on cell cycle progression, morphogenesis and the related events for construction of cell wall architecture in *Schizosacchromyces pombe*. FPy predominantly inhibited the growth of the yeast cells after various cycles of cell division so that cells were arrested at the phase of separation into daughter cells accompanying morphological changes to swollen spherical cells at 24 h of incubation. FPy-treated cells were osmotically stable but were susceptible to the lytic action of (1, 3) β-D-glucanases, and characterized by serious damages to the cell wall architecture as represented by a rough and irregular surface outlook. The isolated cell wall fraction gave a similar hexose composition with or without FPy treatment, suggesting that FPy did not inhibit the synthesis of each cell wall polysaccharide. FPy was permissive for the extracellular accumulation of amorphous cell wall materials and septum development in protoplasts, but absolutely interfered with the following morphogenetic process for construction of the rod-shaped cell wall architecture. Our results suggest the inhibitory activity of FPy on the spatial control over the assembly of cell wall polysaccharides.

Key words: cell wall, isoprenoid, morphogenesis, polysaccharide, *S. pombe*.

Abbreviations: CA, cytochalasin A; CFU, colony forming unit; FOH, farnesol; FNH_2, farnesylamine; FPy, 1-farnesylpyridinium; MIC, minimum growth inhibitory concentration; ROS, reactive oxygen species; GPy, 1-geranylpyridinium; GGPy, 1-geranylgeranylpyridinium; LPy, 1-laurylpyridinium.

The isoprenoid farnesol (FOH, Fig. 1) causes various growth inhibitory effects when exogenously added to cells of bacteria (*1*), archaea (*2*), yeasts (*3–5*) and mammals (*6–9*). The addition of FOH in medium results in the leakage of intracellular K^+ in cells of *Staphylococcus aureus*, suggesting its plasma membrane disruptive damage (*1*). FOH inhibits the biosynthesis of mevalonate from acetate, which is a common precursor of isoprenoid synthesis in cells of *Halobacterium volcani* (*2*). On the other hand, FOH induces apoptosis in mammalian cells and the mechanism of such a cell death induction was partly elucidated on the basis of its promotive effect on degradation of 3-hydroxy-3-methylglutaryl-CoA reductase, which is a rate-limiting enzyme of the isoprenoid biosynthetic reactions or by its inhibitory activity on the phosphatidylcholine biosynthetic reaction (*6*, *7*). The recent studies on FOH-induced apoptosis rather support its relation to the inhibition of protein kinase C–dependent or phospholipase D–dependent signal transduction (*8*, *9*). Unlike the case with other organisms, however, FOH-induced growth inhibition of *Saccharomyces cerevisiae* cells is elucidated by an impairment of the mitochondrial respiratory function leading to reactive oxygen species (ROS) generation (*3–5*). Farnesylamine (FNH_2, Fig. 1), which lacks the terminal hydroxyl group to be pyrophosphorylated, inhibits another reaction of the isoprenoid metabolism such as farnesylation of p21Ras in *ras*-transformed mammalian cells (*10*, *11*). FNH_2 also inhibits the growth of *S. cerevisiae* cells by accelerating ROS production, but its promotive effect on oxidative stress induction depends directly on enzymatic oxidation of its terminal amino group by amine oxidase in the yeast mitochondrial fraction (*12*). These findings suggest that FOH can exhibit a variety of activities owing to its terminal structure and a kind of organism tested.

1-Farnesylpyridinium (FPy, Fig. 1) is a novel analog of FOH in which the acyclic isoprenoid hydrocarbon cannot serve as a precursor or substrate in any of the possible reactions in isoprenoid metabolism. In our previous study, FPy was found to show greater and more unique tumor suppressive potency than FOH in human promyelocytic leukemia HL-60 cells (*13*). The unusual morphological profile of FPy-induced apoptotic event in the mammalian cells could be elucidated by a newly generated cytochalasin-like activity of the analog that can prevent actin organization or promote its disorganization. FPy inhibited the production of a flavor compound such as

*Present address: Research Center, Earth Biochemical Co., Ltd., 923 Kagasuno, Kawauchicho, Tokushima 771-0130.

†To whom correspondence should be addressed. Phone: +81-6-6605-3163, Fax: +81-6-6605-3164, E-mail: tanakato@sci.osaka-cu.ac.jp

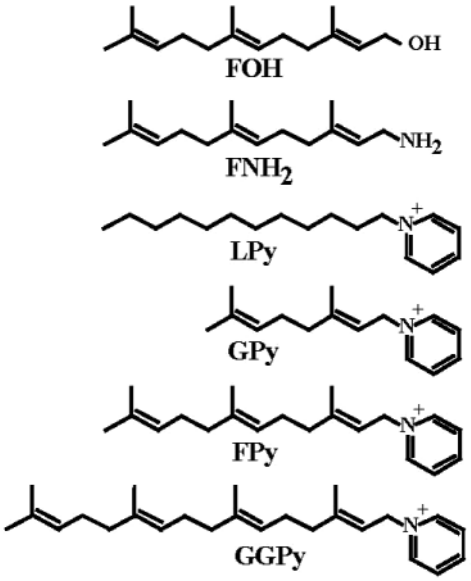

Fig. 1. **Structures of FOH, FNH_2, LPy, GPy, FPy, and GGPy.**

isoamylacetate by a sake yeast at a lower concentration than required for inhibition of the yeast cell growth and one of the FPy-resistant mutants was characterized by a predominant capability of isoamylacetate production (*14*). This was attributed to the elevation of alcohol acetyltransferase activity in the mutant strain, which is under the control of Ras/cAMP pathway, cellular amino acid metabolism and a protein kinase Sch9p (*15*, *16*). FPy is thus expected to affect actin-dependent events in yeast cells since Ras is involved in polarized cell growth of the organism in which the cytoskeletal protein is distributed to the points of growth and cell wall deposition (*17*, *18*).

In the present study, we examined the growth inhibitory activity of FPy widely against yeasts and filamentous fungi, and the analog was found to predominantly inhibit the growth of the fission yeast *Schizosaccharomyces pombe* to a greater extent. FPy lost the activity of oxidative stress induction such as mediated by FOH an FNH_2. On the other hand, FPy-treated cells were characterized by the damages to the later morphogenetic process of cell wall materials, but not the initial step for the synthesis and deposition of cell wall polysaccharides. The characteristic growth inhibitory activity of FPy absolutely depended on its hybrid structure consisting of farnesyl moiety and pyridine ring. However, the yeast isoprenoid metabolic pathway was not considered to be a target of FPy-induced morphological change. We could confirm the failure in the construction of rod-shaped cell wall architecture in spite of accumulation of amorphous cell wall materials and septum development in FPy-treated protoplasts. We therefore consider the possibility that FPy inhibits the extracellular event such as spatial control over the assembly of cell wall polysaccharides.

MATERIALS AND METHODS

Microbial Strains and Media—Antifungal activities of FOH, FPy, and the related compounds were compared by measuring their minimum growth inhibitory concentrations (MICs) in the 2-fold broth dilution method according to our previously described method (*19*, *20*). The microbial strains used were as follows: *Candida albicans* IFO 1061, *C. utilis* OUT 6020, *Saccharomyces cerevisiae* X2180-1A(a), *S. cerevisiae* IFO 0203, *S. pombe* L972 h^-, *S. pombe* SA21 h^+, *S. pome* 0342, *Rhodotorula mucilaginosa* IFO 0001, *Aspergillus niger* ATCC 6275, *Penicillium chrysogenum* IFO 4626, *Mucor mucedo* IFO 7684, and *Rhizopus oryzae* IFO 4766. *S. pombe* FY15563 h^{90} *leu*1 *ura*4 *lys1*$^+$::*pnmt1-GFP-atb2*$^+$ was obtained from Yeast Genetic Resource Center (Osaka City University, Japan) (*21*). Cells of yeast strains were grown in YPD medium consisting of 1% yeast extract, 2% peptone, and 2% glucose, whereas those of filamentous fungi were grown in 2.5% malt extract medium at 30°C for 2 days.

Measurement of Yeast Cell Growth—Unless stated otherwise, *S. pombe* L972 h^- cells were grown overnight in YE medium containing 1% yeast extract and 2% glucose at 30°C with vigorous shaking and inoculated into freshly prepared medium to give an initial cell density of approximately 10^6 cells/ml. The cells were then grown in the presence or absence of FPy with vigorous shaking at 30°C, and portions were withdrawn at various times to measure the cell density at the wave length of 610 nm and to measure the colony forming units (CFU) as the viable cell number.

Measurement of ROS Production—Cells of *S. cerevisiae* X21801-1A(a) and *S. pombe* L972 h^- were grown in YPD medium with vigorous shaking at 30°C and were harvested by centrifugation. Cells from an overnight culture were harvested by centrifugation, suspended in YPD medium to obtain a density of 10^7 cells/ml and incubated with the addition of 40 μM 2′,7′-dichlorodihydrofluorescein diacetate (DCFH-DA) at 30°C for 60 min. Intracellular ROS production was then assayed by a method dependent on intracellular deacylation and the oxidation of DCFH-DA (*3*).

Flow Cytometric Analysis and Fluorescence Microscopy—Cells were inoculated in YE medium at a density of 10^7/ml and grown at 30°C for 24 h with or without 25 μM FPy. Approximately 10^7 cells were collected by centrifugation, washed once with water, fixed in 70% ethanol, and processed for flow cytometry (*22*). Nuclear staining was done with DAPI (4′,6-diamidino-2-phenylindole), and the stained specimen was observed under a fluorescence microscope, as described by Kashiwazaki *et al.* (*23*). Actin staining was done with rhodamine-phalloidin according to the method of Kobori *et al.* (*24*) and cells were observed under a fluorescence microscope with excitation at 540 nm and emission at 565 nm. *S. pombe* FY15563 was used for visualization of microtubules with the aid of the fluorescence from GFP-α-tubulin (*21*).

Electron Microscopy—Cells were inoculated in YE medium at a density of 10^7/ml and grown at 30°C for 24 h with or without 25 μM FPy. The cells were then fixed with 2% glutaraldehyde and postfixed overnight with 1% potassium permanganate in 0.1 M phosphate buffer (pH 7.2). The fixed cells were embedded in 2% agar and dehydrated through a graded ethanol series. The specimens were embedded in Epon 812, and stained with 1% uranyl acetate and then with Reynolds' solution. Ultra-thin sections were observed under a Hitachi H-7000 electron microscope at 100 kV.

Assay of Cell Lysis—Cells were inoculated in YE medium with or without 25 μM FPy at a density of 10^7/ml and grown at 30°C for 24 h and then washed twice with 10 mM sodium citrate buffer (pH 7.0). FPy-treated and untreated cells were suspended in 5.0 ml of the buffer to give an A_{610} value of 0.6. The cell suspensions were vigorously shaken with or without the addition of 720 μg each of Zymolyase and the lysing enzyme from *Stachybotrys elegans* at 30°C, and the enzyme-dependent cell lysis was monitored by measuring the turbidity drop.

Analysis of Cell Wall Hexose Composition—The cells were inoculated in YE medium with or without 25 μM FPy at a density of 10^7/ml and grown at 30°C for 24 h. The cell wall fractions were isolated and analyzed for their hexose composition by the method of Dallies *et al.* (*25*). Briefly, the cells were disrupted by repeated vortexing of the cell suspension in the presence of 10 mM Tris-HCl buffer (pH 8.0) and glass beads (0.45–0.55 mm) until more than 95% of the cells were broken. After separation of the glass beads by repeated centrifugation and washing with the buffer, the cell debris in the supernatant and washings were combined, centrifuged to precipitate the cell wall as a pellet, and purified by repeated centrifugation at 5,400 × *g* and washing with distilled water. The cell walls were then hydrolyzed with 2 N H_2SO_4 at 100°C for 4 h in a sealed tube after pretreatment with 72% H_2SO_4. Hexoses in each acid hydrolysate were analyzed as the corresponding alditol acetates by conventional gas-liquid chromatography.

The isolated cell wall fractions (10 mg) were incubated with 720 μg of the lysing enzyme from *S. elegans* in 1.0 ml of 10 mM sodium citrate buffer (pH 7.0) at 30°C for 24 h. Curdlan was also subjected to enzymatic hydrolysis under the same conditions. A 30-μl portion of each supernatant was spotted onto a silica gel plate (Kiesel gel 60, Merck). After development twice with a mixture of butanol, pyridine and water (8:1:1, v/v) as a solvent, sugars on the plate were detected by dipping it into ethanol containing 10% sulfuric acid and heating at 120°C for 10 min.

Assay of Protoplast Reversion—Protoplasts of *S. pombe* cells were prepared by the method of Kobori *et al.* with a slight modification (*24*). The cells were inoculated in YE medium at a density of 10^7 cells/ml, and grown at 30°C for 16 h, and harvested by centrifugation. The cells were washed with E buffer (50 mM sodium citrate, 100 mM sodium phosphate, pH 6.0), and suspended in E buffer containing 1.2 M sorbitol at 5×10^7 cells/ml. The cell suspension was incubated with the addition of lysing enzyme from *Trichoderma harzianum* at a concentration of 5 mg/ml at 30°C for 90 min with gentle agitation. The protoplasts formed were harvested by centrifugation and washed twice with E buffer containing 1.2 M sorbitol. The protoplasts were then suspended in YE medium containing 1.2 M sorbitol at a density of 10^7 cells/ml and were incubated with or without the addition of FPy at 30°C with gentle agitation. At various time intervals, portions of each suspension were collected by centrifugation and fixed with 1% glutaraldehyde in phosphate-buffered saline (PBS) at room temperature for 20 min. The fixed samples were washed twice with PBS and suspended in PBS which contained calcofluor white M2R at 0.2 mg/ml, and subjected to a 30-min incubation in the dark. After two washes with PBS, the protoplasts were suspended in PBS and observed under a phase contrast-fluorescence microscope with excitation at 352 nm and emission at 461 nm.

Assay of Protein Farnesylation—Exponentially growing cells were harvested by centrifugation, washed, and suspended in 100 mM Tris-HCl buffer (pH 7.5) containing 50 mM nonidet p-40, 100 mM NaCl, 5 mM $MgCl_2$, 100 mM NaF, 4 mM benzamide, 12 μM leupeptin A, and 6 μM dithiothreitol. The cells were disrupted by repeated vortexing of the cell suspension in the presence of glass beads (0.45–0.55 mm). After separation of the glass beads and insoluble materials by centrifugation, the supernatant was used for the assay of protein farnesylation according to the method of Kothapalli *et al.* (*10*). The supernatant containing farnesylpyrophosphate (5.5 kBq) as a substrate in a total volume of 100 μl was incubated with or without addition of 100 μM FPy at 30°C for 1 h. The farnesylated proteins were then precipitated by the addition of 5 volumes of 30% trichloroacetic acid and 4% SDS, and were kept at 0°C for 30 min. The precipitates were collected on a glass fiber filter by filtration and washed 3 times with 1 ml of 30% trichloroacetic acid containing 4% SDS. After drying overnight at room temperature, the radioactivity on the filter was measured with 5 ml of cocktail consisting of 5% 2,5-diphenyloxazol and 0.03% 1,4-bis 2-(5-phenyloxazol)-benzene in a liquid scintillation counter.

Syntheses of Isoprenoid Analogs—FNH_2 and FPy were synthesized as previously reported (*12*, *13*). 1-Geranylpyridinium (GPy, Fig. 1) and 1-geranylgeranylpyridinium (GGPy, Fig. 1) were synthesized by exactly following the method of FPy synthesis using each of geranylchlolide and geranylgeranylcholide, respectively, as a donor of prenyl moiety (*13*). Geranyl chloride was a product of Sigma. Geranylgeranyl chloride was prepared from geranylgeraniol with *N*-chlorosuccinimide and dimethyl sulfide according to the method of Davisson *et al.* (*26*). The spectral data of GPy and GGPy were taken on a Bruker DRX-600 spectrometer in chloroform-d_1 and are summarized in addition to those of FPy as follows. Solvent signals at δ 7.24 ppm (^{1}H) and at δ 77.0 ppm (^{13}C) were used as internal standards, and chemical shifts are expressed in δ values.

GPy: ^{1}H-NMR (600 MHz, $CDCl_3$) δ 1.584 (s, 3H), 1.664 (s, 3H), 1.897 (s, 3H), 2.145 (brs, 4H), 5.023 (brt, 1H), 5.501 (brt, 1H), 5.593 (d, J = 6.3 Hz, 2H), 8.104 (brt, 2H), 8.502 (t, 1H), 9.257 (brd, 2H). ^{13}C-NMR (150 MHz, $CDCl_3$) δ 17.21, 17.78, 25.72, 26.01, 39.52, 59.48, 115.68, 123.16, 128.42, 132.45, 144.51, 145.30, 148.63. The HR-EIMS spectrum value of *m/z* 216.3 (M^+) detected with GPy coincided with *m/z* 216.3419 calculated for $C_{15}H_{22}N$.

FPy: ^{1}H-NMR (600 MHz, $CDCl_3$) δ 1.522 (s, 6H), 1.626 (d, J = 1.2 Hz, 3H), 1.858 (d, J = 1.0 Hz, 3H), 1.891 (dd, J = 8.1, 6.8 Hz, 2H), 1.962 (dt, J = 7.6, 7.1 Hz, 2H), 2.079 (d, J = 3.2 Hz, 2H), 2.082 (s, 2H), 4.995 (dt, J = 7.1, 1.5 Hz, 1H), 5.010 (dt, J = 6.6, 1.5 Hz, 1H), 5.467 (t, J = 8.0 Hz, 1H), 5.593 (d, J = 7.5 Hz, 2H), 8.079 (dd, J = 6.6, 5.7 Hz, 2H), 8.467 (tt, J = 7.8, 1.0 Hz, 1H), 9.380 (d, J = 5.6 Hz, 2H). ^{13}C-NMR (150 MHz, $CDCl_3$) δ 17.24, 17.58, 19.00, 25.55, 26.02, 26.64, 39.48, 39.60, 59.21, 115.72, 122.92, 124.04, 128.30, 131.34, 136.04, 144.69, 145.06, 148.45. The HR-EIMS spectrum value of *m/z* 284.5 (M^+) detected with FPy coincided with *m/z* 284.4589 calculated for $C_{20}H_{30}N$.

GGPy: ^{1}H-NMR (600 MHz, $CDCl_3$) δ 1.556 (s, 9H), 1.640 (s, 3H), 1.880 (s, 3H), 1.919–2.026 (m, 8H), 2.134 (m, 4H),

5.050 (m, 3H), 5.477 (t, J = 7.4 Hz, 1H), 5.628 (d, J = 7.4 Hz, 2H), 8.064 (t, J = 6.6 Hz, 2H), 8.450 (t, J = 7.4 Hz, 1H), 9.358 (d, J = 5.6 Hz, 2H). ^{13}C-NMR (150 MHz, $CDCl_3$) δ 16.00, 16.10, 17.25, 17.65, 25.66, 26.04, 26.61, 26.73, 39.55, 39.68, 39.69, 59.32, 115.60, 122.92, 123.92, 124.30, 128.23, 131.27, 135.15, 136.18, 144.68, 144.96, 148.72. The HR-EIMS spectrum value of *m/z* 352.4 (M^+) detected with GGPy coincided with *m/z* 352.5759 calculated for $C_{25}H_{38}N$.

Chemicals—FOH, cytochalasin A (CA), curdlan, lysing enzyme (*S. elegans*), lysing enzyme (*T. harzianum*), calcofluor white M2R, DAPI, and ketoconazole were purchased from Sigma (St Louis, Mo, USA). Zymolyase 100 T was from Seikagaku Kogyo (Tokyo, Japan). [1-^{3}H]-farnesylpyrophosphate triammonium salt (595 GBq/mmol) was purchased from Perkin Elmer Life Science, Inc (Boston, USA). 1-Laurylpyridinium (LPy, Fig. 1) was a product of Wako Pure Chemical Co. (Osaka, Japan). The other commercially available chemicals were of analytical reagent grade.

RESULTS AND DISCUSSION

Effects of FPy on Cell Growth, ROS Production and Morphogenesis—We first compared the growth inhibitory activities of FPy against filamentous fungi and yeasts with those of FOH using the serial broth dilution method (Table 1). FOH was active against yeast strains other than *C. albicans* and *C. utilis*, and was less active or mostly inactive against strains of filamentous fungi. FPy showed a similar pattern of antifungal activities except that the structural modification resulted in a significant elevation of the growth inhibitory activity against strains of *S. pombe*. FPy was likely to promote ROS production in cells of the fission yeast more effectively than *S. cerevisiae* cells (*3*). Otherwise, a reduced MIC value of FPy against *S. pombe* cells should reflect the generation of a growth inhibitory activity other than the oxidative stress–inducing activity as a result of the structural modification of FOH. As shown in Table 2, FOH promoted ROS production in *S. pombe* cells as effectively as in the *S. cerevisiae* cells at a concentration equivalent to the MIC value (25 μM). FPy exhibited no such activity even at a concentration much higher than the MIC value, indicating the generation of an antifungal activity against the *S. pombe* cells depending on its own hybrid structure.

Table 1. **MICs of FOH and FPy against filamentous fungi and yeasts.**

Test organism	MIC (μM)	
	FOH	FPy
Aspergillus niger ATCC 6275	200	400
Penicillium chrysogenum IFO 4626	100	100
Mucor mucedo IFO 7684	>400	>400
Rhizopus oryzae IFO 4766	400	400
Saccharomyces cerevisiae IFO 0203	50	25
Saccharomyces cerevisiae X2180-1A	50	50
Schizosaccharomyces pombe IFO 0342	25	3.125
Schizosaccharomyces pombe L972 h^-	25	3.125
Schizosaccharomyces pombe SA21 h^+	50	3.125
Candida albicans IFO 1061	400	200
Candida utilis OUT 6020	400	100
Rhodotorula mucilaginosa IFO 0001	50	50

In our previous study, FPy was shown to exhibit a cytochalasin-like activity preventing repolymerization of actin microfilaments that had been depolymerized during the course of apoptotic cell death progression in HL-60 cells (*13*). We therefore examined the mode of action of FPy on *S. pombe* cells using cytochalasin A (CA) as a reference that can most effectively inhibit the yeast cell growth among various cytochalasins tested. CA exhibited a fungicidal activity to reduce the viable cell number in a time-dependent manner at 6.25 μM, as shown in Fig. 2. The pattern of FPy-induced growth inhibition was apparently different from that of the CA-induced one. In medium containing 3.13 μM FPy, the yeast cell growth was successful during the initial 4 h of incubation. The rate of turbidity increase was gradually reduced, followed by a remarkable reduction at 8 h of incubation in coordination with the inhibition of cell division. Although the growth rate was reduced with increasing concentrations of FPy, the yeast cells could initially undergo cell division and were viable up to 24 h of incubation in medium with 25 μM FPy. Such a

Table 2. **Promotive effects of FOH and FPy on ROS production.**

Chemical	Conc. (μM)	ROS production (arbitrary units)	
		S. cerevisiae	*S. pombe*
None	–	423 ± 126	334 ± 121
FOH	25	3,820 ± 263	2,821 ± 190
	50	5,120 ± 370	4,085 ± 481
FPy	25	373 ± 78	420 ± 43
	50	428 ± 110	404 ± 72

Values are means ± SD from triplicate assays.

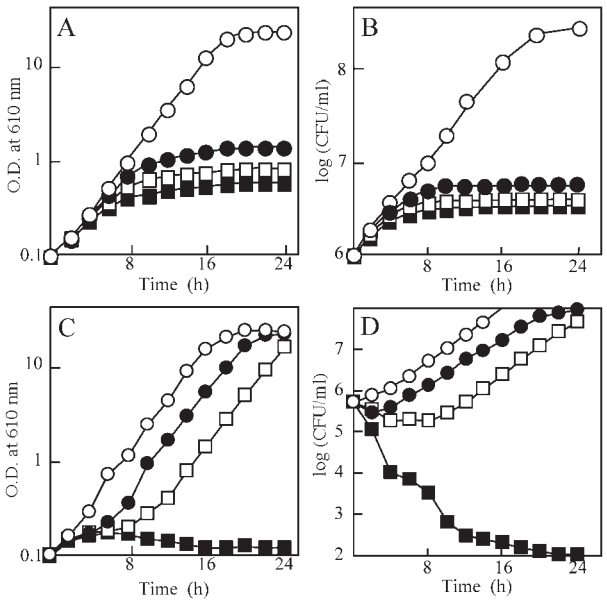

Fig. 2. **Growth inhibitory effects of FPy and CA on *S. pombe* cells.** In (A) and (B), the cells were grown in YE medium containing FPy at 0 (open circles), 3.13 (solid circles), 6.25 (open squares) or 25 μM (solid squares) at 30°C. In (C) and (D), the cells were grown in YE medium containing CA at 0 (open circles), 1.65 (solid circles), 3.13 (open squares) or 6.25 μM (solid squares) at 30°C. Cell growth was measured by the turbidometric assay (A, C) and the viability assay (B, D), in which the viable cell number was expressed as the number of CFU.

delayed growth inhibition pattern of FPy may reflect its action *via* a mechanism other than that directly involved in the cell division or cell cycle progression.

FPy-treated cells slightly increased their turbidity even after cell division was absolutely inhibited, suggesting that FPy-induced cellular damage may be enhanced in a time-dependent fashion so that it could be visualized by microscopic observation. Untreated cells were observed as short rods, representing the typical stationary phase morphology at 24 h of incubation, as shown in Fig. 3. FPy-treated cells showed no distinct cellular damage at 8 h of incubation but cells were mostly observed as enlarged rods each with extraordinary swelling at one or both of the terminal tips at 24 h of incubation. Spherical cells were also observed and were considered to appear as a consequence of the above morphological changes. As expected from the colony-forming ability (Fig. 2B), FPy-treated cells could initiate the polarized growth to obtain normal rod shape when they were incubated in freshly prepared FPy-free medium after harvest from FPy-containing medium by centrifugation at 24 h of incubation (data not shown). Flow cytometric analysis revealed that FPy-treated cells were arrested at the phase having 4c DNA content at 24-h incubation and this agreed with the fact that cells had accomplished nuclear division but failed in separation into daughter cells (Fig. 4, A and B). FPy did not protect against the polymerization of α-tubulin and actin so that these cytoskeletal proteins were visible as filaments and patches, respectively, in the swollen spherical compartment of the cells (Fig. 4, C and D). FPy is likely to inhibit the mechanism of coordinating polarized cell growth and cell division.

Structure–Activity Relationship—Our attention was focused on the molecular component essential for causing FPy-induced morphological change and inhibition of cell division. We thus measured MICs of FPy-related compounds (Fig. 1) and examined their effects on the yeast morphology. FNH_2 inhibited the growth of *S. pombe* cells with a highly increased MIC at 100 μM, and did not cause any remarkable morphological change at this concentration or less. FNH_2-induced growth inhibition of this fission yeast likely depended on the promotive effect on the cellular ROS production, which was evaluated as a cause of its growth inhibitory activity on *S. cerevisiae* cells (*12*). GPy was ineffective in inhibiting the yeast cell growth even at 100 μM. GGPy and LPy showed marked growth inhibitory activities, comparable to that of FPy, with MICs both at 6.25 μM. However, GGPy- and LPy-treated cells were observed with rod-shaped architectures though cells were more elongated than untreated cells after 24-h incubation with GGPy (data not shown). The structure-activity relationship data indicated the requisite of both farnesyl moiety and pyridine ring for FPy-induced events and suggested their dependence on the inhibition of an enzymatic reaction using farnesyl moiety as a substrate or precursor.

cpp1$^+$ encodes the β-subunit of protein farnesyltransferase in *S. pombe* and the mutant cells exhibit rounded or irregular cell morphology (*27*). FNH_2 is rather expected to cause this type of morphological change if this compound inhibits the enzyme in yeast as in the case with its inhibitory activity on the enzyme in mammalian cells (*10*, *11*). FPy may inhibit the protein farnesyltranferase in yeast much more strongly than FNH_2 on the assumption that their MIC values simply reflected the extent of the enzyme inhibition. The cell-free extract of exponentially growing cells contained the enzyme at a specific activity of 350 ± 65 dpm/min/mg protein. FNH_2 significantly inhibited the enzyme activity to 40% of the control level at 100 μM,

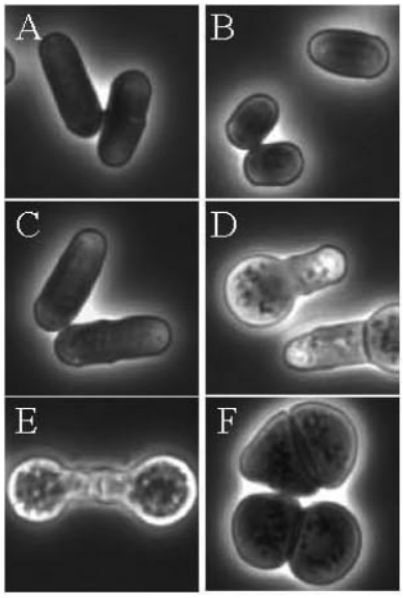

Fig. 3. **Morphological changes of the FPy-treated cells.** The cells were grown in YE medium alone at 30°C for 8 h (A) and 24 h (B) or in YE medium containing 6.25 μM FPy at 30°C for 8 h (C) and 24 h (D, E, F).

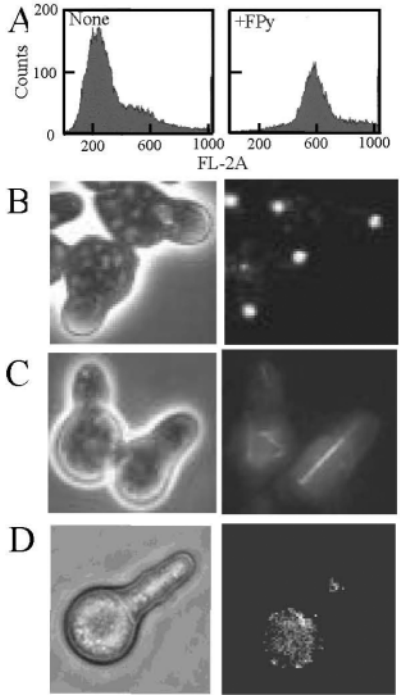

Fig. 4. **Flow cytometric (A) and fluorescence microscopic analyses (B–D) of FPy-treated cells.** The cells were grown in YE medium containing 6.25 μM FPy at 30°C for 24 h and were observed under phase contrast (left) and fluorescence microscope (right) for visualization of nucleus (B), α-tubulin (C) and actin (D).

whereas FPy showed no inhibitory activity at this concentration. We therefore could not attribute the FPy-induced morphological events to its inhibitory activity on protein farnesylation.

Ketoconazole is an inhibitor of isoprenoid biosynthetic pathway leading to ergosterol (*28*). This antibiotic enhances dimorphic transition of hyphal growth to budding growth to form yeast-shaped cells in *C. albicans* at a lower concentration than the lethal concentration, suggesting the relation of the plasma membrane ergosterol content in the yeast morphogenesis. The antibiotic was effective in inhibiting the growth of *S. pombe* cells at 6.25 μM, whereas it was ineffective in causing morphogenetic transition of rod-shaped cells to swollen spherical cells in *S. pombe* at this concentration or less (data not shown). These findings made us to consider the possibility that FPy can more directly affect the yeast cell wall architecture than expected from its molecular structure reminiscent of an inhibitor of isoprenoid biosynthetic pathway.

Effects of FPy on Cell Wall Architecture—Electron microscopic observation demonstrated drastic changes in the overall cell wall architecture of the FPy-treated cells at 24 h of incubation. As shown in Fig. 5, the wall was normally composed of a transparent solid layer that was covered with an electron-dense fibrous layer, in which galactomannoproteins are generally enriched, in the untreated cells (*29*). The FPy-treatment caused a loss of uniform thickness in the overall cell wall architecture as seen from the thicker deposition of cell wall materials at one terminal. The electron-dense layer showed a rough and irregular surface outlook in some images, indicating the failure in the functional assembly or the network formation of the outer cell wall structural polysaccharides. The image showing separation of the wall from the plasma membrane seemed to be made during preparation of the ultra-thin section, but no similar images were observed with the untreated cells. This may indicate a loss of interface interaction between the inner cell wall layer and the periphery of the plasma membrane. The action pattern of FPy on the yeast cell wall architecture rather coincided with that of the myosin inhibitor 2,3-butanedione monooxime (*30*). This inhibitor disorganizes the yeast cell wall at the concentration ineffective for the polymerization status of actin cytoskeleton, resulting in some unusually thick parts lying next to regions where the wall was almost absent.

The inner cell wall layer consisted of (1-3) β-D-glucan, a target of ideal antifungal agents, and (1-3) α-D-glucan (*29*). The inhibition of (1-3) β-D-glucan synthase results in severe lysis of the yeast cells and mutants defective in the enzyme require osmotic stabilization for growth at restrictive temperatures. The treatment with a cell wall digestive enzyme such as Zymolyase can also cause lysis of the yeast cells depending on its (1-3) β-D-glucanase activity (*31*). These findings clearly indicate differences in the mode of action between FPy and an inhibitor of (1-3) β-D-glucan synthase. FPy was not likely to inhibit (1-3) α-D-glucan synthesis as deduced from the action of α-D-glucanase, which produces round protoplasts in liquid medium with an osmotic stabilizer (*32*). As shown in Fig. 6, both FPy-treated and

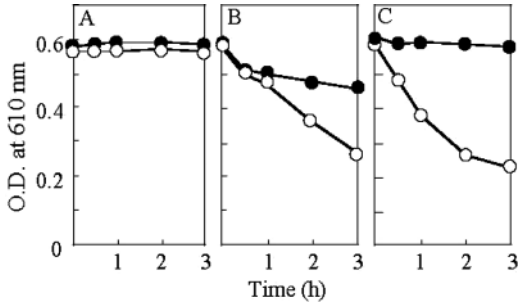

Fig. 6. **Lysis of the cells upon lytic enzyme treatment.** The cells were grown in YE medium alone (solid circles) or YE medium containing 25 μM FPy (open circles) at 30°C for 24 h. After harvesting and washing, the cells were suspended so as to give an A_{610} value of 0.6. The cell suspensions were incubated at 30°C for the indicated times in 10 mM sodium citrate buffer (pH 7.0) alone (A), the buffer containing 720 μg/ml of Zymolyase (B) and the buffer containing 720 μg/ml of the *S. elegans* enzyme (C).

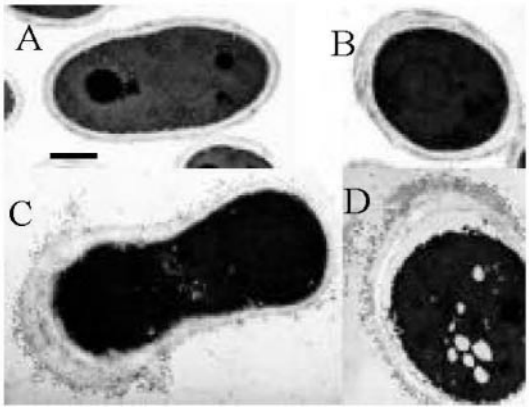

Fig. 5. **Electron microscopic observation of the untreated and FPy-treated cells.** The cells were grown in YE medium alone (A, B) or in YE medium containing 25 μM FPy at 30°C for 24 h (C, D). Bar, 1 μM.

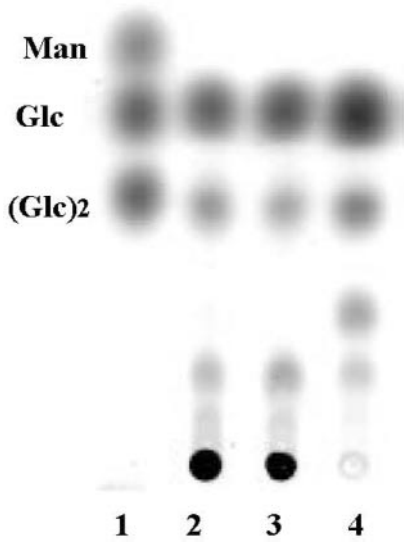

Fig. 7. **Analysis of acid hydrolysis products of isolated cell wall fractions from FPy-treated cells (lane 2), untreated cells (lane 3), and curdlan (lane 4).** In lane 1, 25 μg each of glucose (Glc), laminaribiose (Glc2) and mannose (Man) was spotted and developed as markers.

untreated cells gave no evidence of cell lysis even when incubated in the buffer solution without any osmotic stabilization. The result means that FPy-treated cells still contained enough (1-3) β-D-glucan and (1-3) α-D-glucan for osmotic stability. However, Zymolyase could more rapidly achieve the lysis of FPy-treated cells than untreated cells, suggesting that FPy-treatment resulted in the loss of network formation between (1-3) β-D-glucan and other cell wall polysaccharides. Such FPy-induced damage on the spatial arrangement of cell wall polysaccharides was more markedly demonstrated by the lytic action of the lysing enzyme from *S. elegans* (*33*).

We then compared the enzymatic hydrolysis pattern of the isolated cell wall fractions from FPy-treated and untreated cells in order to find out whether FPy-treatment caused any structural alteration of the (1-3) β-D-glucan in favor of acceleration of enzyme-dependent cell lysis. As shown in Fig. 7, the *S. elegans* enzyme could effectively hydrolyze curdlan, a linear (1-3) β-D-glucan, to produce laminaribiose, laminaritriose and laminaritetraose in addition to glucose, representing a typical action pattern of (1-3) β-D-glucanase. The enzyme could partially digest the isolated cell wall fractions from FPy-treated and untreated cells in an almost identical fashion. Although laminaritriose was scarcely detected in each of the hydrolysates, the action patterns of the *S. elegans* enzyme revealed (1-3) β-D-glucanase to be an enzyme responsible for hydrolysis of the isolated cell wall fractions and for the lysis of FPy-treated cells. The data obtained above supported the idea that FPy caused no remarkable alteration in the structure of (1-3) β-D-glucan but altered the overall cell wall architecture so that the enzyme could more easily attack (1-3) β-D-glucan of the inner cell wall constituent *in vivo*.

Table 3. **Yields of cell walls and their hexose compositions.**

Chemical	Cell wall[a] *(%)*	Hexose (%)[b]		
		Glucose	Mannose	Galactose
None	29.5 ± 5	82.1 ± 0.8	8.3 ± 0.2	9.6 ± 0.6
25 μM FPy	25.4 ± 4	83.7 ± 0.4	7.5 ± 0.3	8.8 ± 0.5

Values are means ± SD from triplicate assays.
[a]Percentage of total dry cells. [b]Percentage of total hexose.

The outer galactomannan layer may affect the susceptibility of the inner (1-3) β-D-glucan layer against the lytic action of the *S. elegans* enzyme. A papulacandin-resistant mutant, JC6, which is characterized by round shape with a low amount of galactomannan, showed increased sensitivity to Novozyme compared to the parent cells (*34*). The cell wall was considerably thicker than that of the parental strain in spite of a lower galactose and mannose content upon acid hydrolysis of the isolated cell wall fraction. It was examined whether the FPy-treatment can affect the galactomannan content by analyzing the hexose composition of its acid hydrolyzate. As shown in Table 3, the cell walls were isolated at a slightly lower yield from the FPy-treated cells than the untreated cells. The difference does not mean that the total quantity of cell wall materials per cell is lower in the FPy-treated cells, since the ratio of the cell number to total dry matter should also be lower in FPy-treated cells because of their increased cell size. The walls from the FPy-treated cells were characterized by a galactose and mannose content slightly lower than those of the untreated cells, but the hexose composition was apparently in a normal range when compared with the values in the above reports. This result ruled out the idea that FPy selectively inhibited one of the enzyme reactions involved in the synthesis of these cell wall structural polysaccharides.

Effects of FPy on Cell Wall Regeneration in Protoplasts—FPy may have its target in a step involved in the proper assembly of the cell wall polysaccharides. We

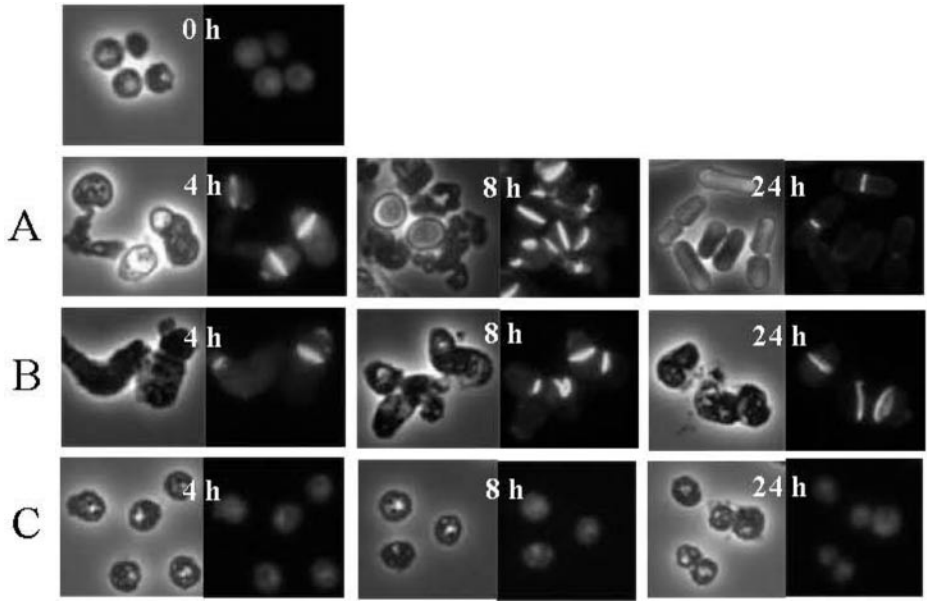

Fig. 8. **Effects of FPy and CA on the cell wall regeneration of reverting protoplasts.** Protoplasts were incubated in regeneration medium alone (A), the medium containing 25 μM FPy (B) and the medium containing 6.25 μM CA (C) at 30°C for the indicated times. The fixed samples were stained with calcofluor white M2R and were observed under phase contrast microscope (left) and fluorescence microscope (right).

finally examined the effect of FPy on the process of cell wall regeneration in reverting protoplasts using CA as an inhibitor of protoplast reversion. As shown in Fig. 8, protoplasts regenerated amorphous cell wall materials at 4 h of incubation and such a regeneration process was more frequently observed together with septum development at 8 h of incubation in the control assay. Protoplasts had already reverted into vegetative cells with a rod-shaped cell wall architecture and mostly accomplished the exponential phase of growth by 24 h of incubation. CA-treated protoplasts were absolutely protected against the regeneration of cell wall materials and septum formation. FPy-treated protoplasts showed a similar pattern of cell wall regeneration to those of untreated protoplasts at up to 8 h of incubation but failed to initiate the following morphogenetic step for construction of rod-shaped cell wall architecture. The analog did not inhibit septum development as seen from the appearance of a brightly stained architecture within the cells, meaning that FPy allows the intracellular event essential for the deposition or assembly of the cell wall polysaccharides.

The isoprenoid FOH lost the original activity of oxidative stress induction as a result of the structural modification whereas the hybrid structure of farnesyl chain and pyridine ring newly generated a predominant growth inhibitory activity on *S. pombe* cells. FPy-induced events in yeast cells may have a relation to its cytochalasin-like activity on mammalian cells but its mode of action on the yeast cell growth was apparently distinguished from that of CA in yeast cells. FPy apparently affected the process for proper assembly of cell wall polysaccharides rather that the process of their syntheses or deposition. Css1p is a plasma membrane-associated inositolphosphosphingolipid-phospholipase C in *S. pombe*. (*35*). *css1* temperature-sensitive mutants are characterized by large depositions of α- and β-glucan inside the cells along with the inhibition of cell division, predicting the existence of an enzyme or process essential for the coordination of the yeast cell wall construction and cell division in response to the sphingolipid metabolism. Our results suggest that FPy inhibits the extracellular event for spatial control over the assembly of cell wall polysaccharides to build up the entire cell wall architecture. This may also predict the existence of a protein that is essential for the coordination of the yeast cell wall construction and cell division.

The authors are grateful to Hideyoshi Nakamura and Keiko Matsuda for their technical assistance to this work.

REFERENCES

1. Inoue, Y., Shiraishi, A., Hada, T., Hirose, K., Hamashima, H., and Shimada, J. (2004) The antibacterial effects of terpene alcohols on *Staphylococcus aureus* and their mode of action. *FEMS Microbiol. Lett.* **237**, 325–331
2. Tachibana, A., Tanaka, T., Taniguchi, M., and Oi, S. (1996) Evidence of farnesol-mediated isoprenoid synthesis regulation in a holophilic archaeon, *Haloferax volcanii*. *FEBS Lett.* **379**, 43–46
3. Machida, K., Tanaka, T., Fujita, K., and Taniguchi, M. (1998) Farnesol-induced generation of reactive oxygen species via indirect inhibition of the mitochondrial electron transport chain in the yeast *Saccharomyces cerevisiae*. *J. Bacteriol.* **180**, 4460–4465
4. Machida, K., Tanaka, T., Yano, Y., Otani, S., and Taniguchi, M. (1999) Farnesol-induced growth inhibition in *Saccharomyces cerevisiae* by a cell cycle mechanism. *Microbiology* **145**, 293–299
5. Machida, K. and Tanaka, T. (1999) Farnesol-induced generation of reactive oxygen species dependent on mitochondrial transmembrane potential hyperpolarization mediated by F_0F_1-ATPase in yeast. *FEBS Lett.* **462**, 108–112
6. Correll, C.C., Ng, L., and Edwards, P.A. (1994) Identification of farnesol as the non-sterol derivative of mevalonic acid required for the accelerated degradation of 3-hydroxy-3-methyl-glutaryl-coenzyme A reductase. *J. Biol. Chem.* **269**, 17390–17393
7. Miquel, K., Pradines, A., Terce, F., Selmi, S., and Favre, G. (1998) Competitive inhibition of choline phosphotransferase by geranylgeraniol and farnesol inhibits phosphatidylcholine synthesis and induces apoptosis in human lung adenocarcinoma A549 cells. *J. Biol. Chem.* **273**, 26179–26186
8. Voziyan, P.A., Haug, J.S., and Melnykovych, G. (2005) Mechanism of farnesol cytotoxicity: further evidence for the role of PKC-dependent signal transduction in farnesol-induced apoptotic cell death. *Biochem. Biophys. Res. Commun.* **212**, 479–486
9. Taylor, M.M., Macdonald, K., Morris, A.J., and McMaster, C.R. (2005) Enhanced apoptosis through farnesol inhibition of phospholipase D signal transduction. *FEBS J.* **272**, 5056–5063
10. Kothapalli, R., Guthrie, N., Chambers, A.F., and Carroll, K.K. (1993) Farnesylamine, an inhibitor of farnesylation and growth of *ras*-transformed cells. *Lipids* **28**, 969–973
11. Ura, H., Obara, T., Shudo, R., Itoh, A., Tanno, S., Fujii, T., Nishio, N., and Kohgo,Y. (1998) Selective cytotoxicity of farnesylamine to pancreatic carcinoma cells and Ki-*ras*-transformed fibroblasts. *Mol. Carcinog.* **21**, 93–99
12. Tanaka, T., Hijioka, H., Fujita, K., Usuki, Y., Taniguchi, M., and Hirasawa, E. (2004) Oxidative stress-dependent inhibition of yeast cell growth by farnesylamine and its possible relation to amine oxidase in the mitochondrial fraction. *J. Biosci. Bioeng.* **98**, 470–476
13. Hamada, M., Nishio, K., Doe, M., Usuki, Y., and Tanaka, T. (2002) Farnesylpyridinium, an analog of isopreneoid farnesol, induces apoptosis but suppresses apoptotic body formation in human promyelocytic leukemia cells. *FEBS Lett.* **514**, 250–254
14. Hirooka, K., Yamamoto, Y., Tsutsui, N., and Tanaka, T. (2005) Improved production of isoamyl acetate by a Sake yeast mutant resistant to an isoprenoid analog and its dependence on alcohol acetyltransferase activity, but not on isoamyl alcohol production. *J. Biosci. Bioeng.* **99**, 125–129
15. Verstrepen, K.J., Van Laere, S.D.M., Vanderhaegen, B.M.P., Derdelinckx, G., Dufour, J.P., Pretorius, I.S., Winderickx, J., Thevelein, J.M., and Delvaux, F.R. (2003) Expression levels of yeast alcohol acetyltransferase genes *ATF1, Lg-ATF1*, and *ATF2* control the formation of broad range of volatile esters. *Appl. Environ. Microbiol.* **69**, 5228–5237
16. Verstrepen, K.J., Derdelinckx, G., Dufour, J.-P., Winderickx, J., Pretorius, I.S., Thevelein, J.M., and Delvaux, F.R. (2003) The *Saccharomyces cerevisiae* alcohol acetyl transferase gene *ATF1* is a target of the cAMP/PKA and FGM nutrient- signalling pathways. *FEMS Yeast Res.* **4**, 285–296
17. Nurse, P. (1994) Fission yeast morphogenesis. *Mol. Biol. Cell* **5**, 613–616
18. Ho, J. and Bretsher, A. (2001) Ras regulates the polarity of the yeast actin cytoskeleton through the stress response pathway. *Mol. Biol. Cell* **12**, 1541–1555.
19. Akeda, Y., Shibata, K., Ping, X., Tanaka, T., and Taniguchi, M. (1995) AKD-2A B, C and D, new antibiotics from *Streptomyces* sp. OCU-42815: taxonomy, fermentation, isolation, structure elucidation and biological activity. *J. Antibiot.* **48**, 363–368

20. Tanaka, T., Nakayama, K., Machida, K., and Taniguchi, M. (2000) Long-chain alkyl ester of AMP acts as an antagonist of glucose-induced signal transduction that mediates activation of plasma membrane proton pump in *Saccharomyces cerevisiae*. *Microbiology* **146**, 377–384
21. Yamamoto, A., West, R.R., MaIntosh, J.R., and Hiraoka, Y. (1999) A cytoplasmic dynein heavy chain is required for oscillatory nuclear movement of meiotic prophase and efficient meiotic recombination in fission yeast. *J. Cell Biol.* **145**, 1233–1249
22. Vazquez-Novelle, M.D., Esteban V, Bueno, A., and Sacristan, M.P. (2005) Functional homology among human and fission yeast Cdc14 phosphatases. *J. Biol. Chem.* **280**, 29144–29150.
23. Kashiwazaki, J., Nakamura, T., Iwaki, T., Takegawa, K., and Shimoda, C. (2005) A role for fission yeast Rab GTPase Ypt7p in sporulation. *Cell Struct Funct.* **30**, 43–49
24. Kobori, H. Yamada, N., Taki, A., and Osumi, M. (1989) Actin is associated with the formation of the cell wall in reverting protoplasts of the fission yeast *Schizosaccharomyces pombe*. *J. Cell Sci.* **94**, 635–646
25. Dallies, N., Francois, J., and Paquet, V. (1998) A new method for quantitative determination of polysaccharides in the yeast cell wall. Application to the cell wall defective mutants of *Saccharomyces cerevisiae*. *Yeast* **14**, 1297–1306
26. Davisson, V.J, Woodside, A.B., Neal T.R., Stremler, K.E., Muehlbacher, M., and Poulter, C.D. (1986) Phosphorylation of isoprenoid alcohols. *J. Org. Chem.* **51**, 4768–4779
27. Yang, W., Urano, J., and Tamanoi, F. (2000) Protein farnesylation is critical for maintaining normal cell morphology and canavanine resistance in *Schizosaccharomyces pombe*. *J. Biol. Chem.* **275**, 429–438
28. Borgers, M., Van den Bossche, H., and De Brabander, M. (1983) The mechanism of action of the new antimycotic ketoconazole. *Am. J. Med.* **74**, 2–8
29. Arellano, M., Coll, P.M., and Pérez, P. (1999) Rho GTPases in the control of cell morphology, cell polarity and actin localization in fission yeast. *Microsc. Res. Tech.* **47**, 51–60
30. Steinberg, G. and McIntosh, J.R. (1998) Effects of the myosin inhibitor 2,3-butanedione monooxime on the physiology of fission yeast. *Eur. J. Cell Biol.* **77**, 284–293
31. Vrsanska, M., Biely, P., and Kratky, Z. (1977) Enzymes of the yeast lytic system produced by *Arthrobacter* GJM-1 bacterium and their role in the lysis of yeast cell walls. *Z. Allg. Mikrobiol.* **17**, 465–480
32. Moreno, S., Klar, A., and Nurse, P. (1991) Molecular genetic analysis of the fission yeast *Schizosaccharomyces pombe*. *Methods Enzymol.* **194**, 795–823
33. Archambault, C., Coloccia, G, Kermasha, S., and Jabaji-Hare, S. (1998) Characterization of an endo-1, 3-β-D-glucanase produced during the interaction between the mycoparasite *Stachybotrys elegans* and its host *Rhizoctonia solani*. *Can. J. Microbiol.* **44**, 989–997
34. Ribas, J.C., Roncero, C., Rico, H., and Durán, A. (1991) Characterization of a *Schizosaccharomyces pombe* morphological mutant altered in the galactomannan content. *FEMS Microbiol. Lett.* **79**, 263–268
35. Feoktistova, A., Magnelli, P., Abeijon, C., Perez, P., Lester, R.L., Dickson, R.C., and Gould, K.L. (2001) Coordination between fission yeast glucan formation and growth requires a sphingolipase activity. *Genetics* **158**, 1397–1411